International Refereed Journal of Engineering and Science (IRJES)
ISSN (Online) 2319-183X, (Print) 2319-1821
Volume 13, Issue 3 (May.-June. 2024), PP. 01-18

Influence of Amino Substituent's Position on Quinoline for Inhibition of Aluminium Corrosion in Hydrochloric Acid

A.M. Usman[*a], Jaweria Ambreen[*b,d], A.A.Muhammad[*c], Saba Zafar[b], Syafiqah Saidin[d] and Aminu Abdullahi[e]

[a]*Department of Chemistry Federal College of Education (Technical) Bichi, P.M.B.3473, Kano, Nigeria*
[b]*Department of Chemistry COMSATS University Islamabad, Park road, 45550, Islamabad, Pakistan*
[c]*Department of Pure and Industrial Chemistry Bayero University, P.M.B. 3011, Kano. Nigeria.*
[d]*Department of biomedical engineering & Health Sciences, Faculty of Electrical Engineering, Universiti teknologi Malaysia, 81310 UTM, Johor bahru, Malaysia*
[e]Department of biotechnology, Vel Tech Rangarajan, Dr. Sagunthala R&D Institute of Science and Technology, Avadi, Chennai, India-600062.

Abstracts
This study examined the effects of specific aminoquinoline molecules on the inhibition of aluminium corrosion in hydrochloric acid, as well as the effects of the amino group substituent at positions 5, 6, and 8. Experimental measurements using weight loss, EIS, and PDP were conducted. Six aminoquinolines (6-AMQ), seven aminoquinolines (7-AMQ), and eight aminoquinolines (8-AMQ) were used in different mass and temperature conditions with varying HCl concentrations to aid in weight loss. These inhibitors' adsorption properties were discovered to be in line with the long-muir isotherm; physical and chemical processes were all important. Comparatively speaking, 7-aminoquinoline performance was superior to 6- and 8-chloroquinoline, as indicated by the corrosion rate (CR), mass loss, percentage inhibition efficiency (IE), and degree of surface coverage (θ) obtained from the weight loss. For every system, the inhibition progressed at a first-order kinetic pace. The surface morphology and functional group were examined using SEM and FTIR both before and after the corrosion study. The weight loss and the Nyquist plot from the impedance data and parameters both showed the same behaviour. The parameters and the Tafel plot polarisation data both display the same trends. It is discovered that the EIS and PDP results are largely in line with the weight loss results. Every molecule exhibited high corrosion inhibition efficiency. However, compared to the other two molecules, the 7-AMQ molecule inhibits aluminium corrosion more effectively.

Keywords: *aminoQuinoline , aluminium, corrosion, substituents' position, inhibition efficiency*

Date of Submission: 24-05-2024 Date of acceptance: 07-06-2024

I. INTRODUCTION

The use of acidic media in pickling, facility cleaning and descaling is indispensable in so many industries [1] . Hydrochloric acid is a common acidic medium for these purposes because it is more economical, efficient and less troublesome compared to other mineral acids. Even though aluminium is effectively passive in neutral aqueous environment, it is strongly predisposed to corrosion in acidic media even as dilutes as acid rainwater.In the actual facts,Cl^- from various sources including neutral salts, has the ability to cause pitting corrosion at vulnerable spots of passive film-protected non-ferrous metal[2].The protection of aluminium and its oxides against the corrosive action of chloride ions in aqueous medium has been extensively investigated. A great number of inhibitors has been studied, and several number of their actions with regard to corrosion inhibition of aluminium has been reported in the literature[2]. Organic corrosion inhibitors are preferred due to are environmental friendly and effectiveness at wide range of temperatures. The efficiency of organic inhibitor depends on the size of the organic molecule, aromaticity, type and number of bonding atoms or groups in the molecule (π and σ bonds), nature and surface charge, the distribution of charge in the molecule and the type of aggressive media[3]. The presence of polar functional groups with S, O or N atoms in the molecule, heterocyclic compounds and pi electrons present in the molecule also increases the efficiency of these organic corrosion inhibitors[3]. The use of computational chemistry such as density functional theory (DFT), molecular dynamic simulation (MD), Monte carlo (MC) simulation and quantitative structure-activity relationship (QSAR) modelling has been applied for study of corrosion inhibition properties of organic molecules. Aromatic rings has

mostly been regarded as the zones through which certain inhibitors can protect etching of metals. Functional group attached to aromatic ring also has great role in corrosion inhibition of metals generally[4].

Aminoquinolines are nitrogenous bicyclic heterocyclic compounds with molecular formula of $C_9H_8N_2$, as such it is expected to show a reasonable good effectiveness against metallic corrosion because of its association with high electron density (10-π and 2-nonbonding electrons). Quinoline derivatives containing polar substituent such as amino group ($–NH_2$) can effectively adsorb and form highly stable chelating complexes with surface metallic atoms through coordination bonding[5]. The available studies for corrosion inhibition of quinoline molecules focuses on the nature and type of functional groups (being substituted or non-substituted) attached to the molecule in use. To our knowledge, this is the first investigation for the effect of position of substituent groups in corrosion inhibition for aluminium in acidic environment[6]. However, aside from aromaticity, functional group and the type of substituent, corrosion inhibition efficiency of heterocyclic compound can also be influence by the nature and position of substituent attached to the molecule. This study is aimed at justifying the claim, being very scanty or non from the literature.

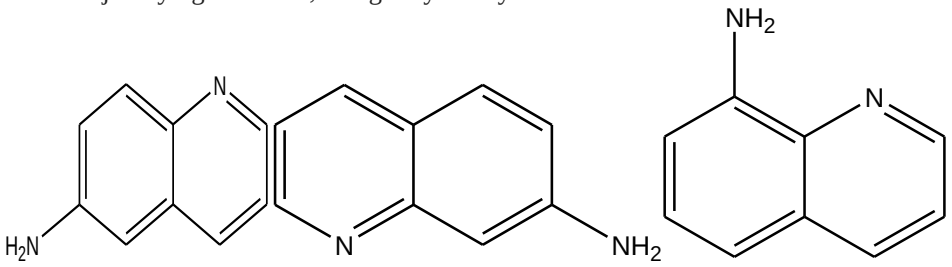

6-aminoquinoline 7-aminoquinoline 8-aminoquinoline

II. Materials And Methods

2.1 Materials

The inhibitors which are the aminoquinolines {6-aminoquinoline(6-AMQ),7-aminoquinoline(7-AMQ) and 8-aminoquinoline(8-AMQ)} three in number, were obtained from the Aldrich Chemical Co. Ltd, (Gillingham Dorset - England), all with 99% purity. The inhibitors were used without further purification. Other materials are the distilled water, ethanol; with 96%, purity, hydrochloric acid; with 37% purity and specific gravity of 1.175-1.185 g/20^{o}C and diethyl ether; with 99.5% purity and specific gravity of 0.713-0.714. The aluminium plate used in this study composed of 98.9% Al , 0.5% Fe and 0.48% Si with traces of other elements which includes: Ti, V, Mn, Ni Cu, Gaetc in negligible amount, falling within the class of wrought aluminium. The metal coupons used in this experiment were mechanically cuts and optimized (5.0cm × 3.0cm × 0.11cm) degreased in ethanol, rinsed in acetone, air dried and preserved in moisture free desiccators prior to corrosion study. Doubly distilled water was used to prepare test solution of the corrodent by diluting 37% HCl from Sigma-Aldrich.

2.2 Mass Loss Measurement

The Metals coupons (5.0 cm × 3.0 cm × 0.11 cm) obtained was firstly weighed, suspended with the aid of Pyrex glass hooks tightened on a rod horizontally placed end to end held by retort stands such that 4.0cm × 3.0cm of the test metal is immersed each in 80ml of 0.2M, 0.4M and 0.6M HCl solution containing different concentrations of inhibitor (0.0, 0.2, 0.4, and 0.6 g/L) . Contact was allowed for 5 h at 303, 313 and 323K. The coupons were then withdrawn at predetermined intervals of time, washed, rinsed in diethyl ether, dried and reweighed. The mass losses was recorded. The above procedure was tested for all the three quinolinederivatives[6]. Each experiment was carried out three times (Femi and Habiba 2015).The mass measurements was performed on Mettler FA2004 electronic balance. From the mass loss data, corrosion rate (CR, in $gh^{-1}cm^{-2}$), the degree of surface coverage (θ) and Inhibition efficiency I (%) were computed using Equations[7] :

$$\text{Weight Loss} = W_1 - W_2 \quad (3.1)$$

$$\theta = 1 - \frac{W_1}{W_2} \quad (3.2)$$

$$\%\ IE = \left(1 - \frac{W_1}{W_2}\right) \times 100 \quad (3.3)$$

$$CR\ (gh^{-1}cm^{-2}) = \frac{\Delta W}{At} \quad (3.4)$$

Where W_1 is the initial masses (g) of Al and W_2 is the final mass after time t, θ is the degree of surface coverage of the inhibitor, A is the area of the Al coupon (cm2), t is the immersion time (h).

2.3 Electrochemical Measurements

2.3.1 Impedance Measurement

Electrochemical Impedance tests was carried out at 303 ± 1K in a three electrode cell using a Gamry interface 5000E potentiostat (Louis Drive Warminster, PA 18974, USA) equipped with complete Gamryframeworkversion 7.9.0 and GamryEcchm Analyst version7.9.0 , with V_3 Studio software over a frequency range of 100 kHz - 10 mHz, with a signal amplitude of 5mV. A graphite rod was used as counter electrode and Ag/AgCl electrode was used as the reference electrode. The latter was connected via a Luggin's capillary. Each test was runs in triplicate. Measurements was performed in 0.4 M acid solutions containing 0.4g/L mass of the test inhibitors in aerated and unstirred solutions after 30 minutes immersion in the test solutions[8]. The working electrodes was prepared from square sheets of aluminium with $1cm^2$ of the area exposed to the test solution. Origin lab software was used for the data handling which gives the Nyquest plot of each system. The charge transfer resistance values were obtained from the diameter of the semi circles of the Nyquist plots. The inhibition efficiencies of the inhibitors was also calculated from the charge transfer resistance values [9].

2.3.2 Potentiodynamic Polarization

Potentiodynamic polarization studies was performed in 0.4 M HCl at 303 K using a Gamry interface 5000E potentiostat (Louis Drive Warminster, PA 18974, USA) equipped with complete Gamryframeworkversion 7.9.0, having an acquisition system installed with NOVA software package version 1.8 and a three-electrode electrochemical cell: the metal coupons of surface area 1 cm^2 as working electrode, an Ag/AgCl reference electrode and a graphite counter electrode. Aluminium samples for electrochemical experiments were of dimension 1.0 cm × 1.0 cm ×0.11 cm. These were subsequently sealed with epoxy resin in such a way that only one square surface of area 1.0 cm^2 was left uncovered. The exposed surface was degreased in acetone, rinsed with distilled water, and air dried. The aluminium metal was polarized between –1,000 and 2,000 mV at a certain scan rate of 0.333 mV s^{-1} and 303K. From the polarization test data for inhibited aluminium in acid medium,the electrochemical parameters such as Tafel slopes, corrosion potential, corrosion current and corrosion rate were calculated. The linear region of anodic and cathodic curves was extrapolated with 0.0016V/sec scan rate. From the Tafel analysis; corrosion current density, corrosion rate, linear polarization resistance and corrosion potential were obtained in a static solution [10]. The inhibition efficiency IE (%) was also computed. Each test was runs in triplicate. Measurements was performed in 0.4 M acid solutions containing 0.4g/L mass of the test inhibitors(Oguzie*et al*, 2015). The inhibition efficiency (%IE) was deduced from the linear polarization resistance (LPR) and potentiodynamic polarization-corrosion rate (PP-CR) which was used as criteria for assessment of corrosion resistance of aluminium in corrosive environments using the following equations:

$$\%IE = \frac{CR_o - CR}{CR_o} \times 100 \qquad 3.5$$

Where $CR_o$and CR are corrosion rates of the materials in the presence and absence of inhibitors respectively[11].

2.4 Surface characterization

To understand the type and nature of corrosion on the aluminium, the resulting surfaces before and after corrosion, were examined on PhenomProX model (Netherlands) scanning electron microscope at accelerating voltages of 5.00kV. Infrared spectra of the adsorbed inhibitors were recorded using SHIMADZU FTIR-8400S Fourier Transform Infrared Spectrometer (FTIR) over a frequency range of 400-4000cm^{-1}. Elemental analysis of aluminium test plates was performed on Mini pal 4 PW 4030 energy dispersive X-ray fluorescence spectrometer (EDXRF) installed with Mini Pal analytical software. The specimens were stimulated by a potential of 30 kV and a current of 1 mA for 10 min.

III. Results and Discussion

3.1 Weight Loss Analysis

The corrosion inhibition performance profile of 6-AMQ, 7-AMQ and 8-AMQ systems for the anti-corrosion effect on aluminium via weight loss experiment is shown in the figures 3.1 to 3.5 below. Starting with figure 3.1, the profile indicates a progressive decrease in weight loss with increase in the inhibitors masses (g/L) at 303K for all the three system (6-AMQ/0.2MHCl on Al, 7-AMQ/0.2MHCl on Al and 8-AMQ/0.2MHCl on Al) concurrently under the same condition. The vertical height of the bars in figure 3.1 to 3.3 is a function of the amount of weight lost by the aluminium in test for the blank and the inhibited case for all the system. This is in

agreement with the fact that the presence of inhibitor molecule prevent the corrodent molecules (acid) from having full contact with the metal surface such that a barrier has been created in between which could be physically or chemically depending on the adsorption characteristics [15]. Here we can think of it this way : without the inhibitor, the metal surface is like a smooth, flat surface. When the corrodent molecules collide with the metal surface, they have to overcome a lot of resistance to get past the surface and start the corrosion reaction. However, when an inhibitor is introduced, it behave like a small bumps on the surface of the metal. The corrodent molecules can now get a better grip on the metal surface because of the inhibitor molecules. In this situation, the corrodent molecules don't have to overcome as much resistance to start the corrosion reaction. So the presence of the inhibitor molecules effectively reduces the activation energy required for the reaction to occur[16].

The variation of the inhibitors mass from 0.0, through 0.2, 0.4 to 0.6g/L shown in figures 3.1 to 3.3 profile, leads to decrease in mass loss of the aluminium at all temperatures and all corrodent concentration. This is because the increase in the inhibitor mass leads to an increase in the number of inhibitor molecules available to interact with the corrodent molecules and reduce the activation energy[17]. It's just like putting more bumpers on the metal surface to make it easier for the corrodent molecules to attach.

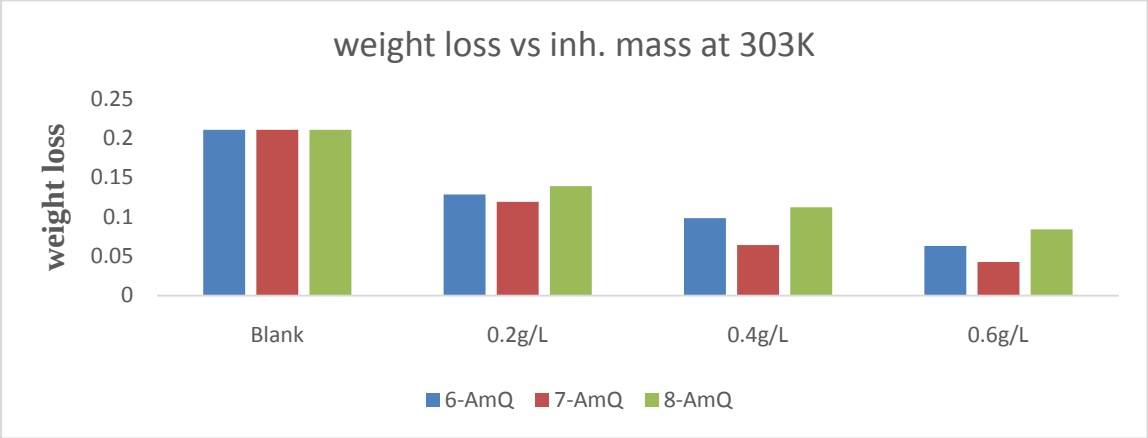

Figure 3.1: Weight loss of aluminium in 0.2M HCl at 303k using 6-AMQ, 7-AMQ and 8-AMQ inhibitors with varying mass for each system.

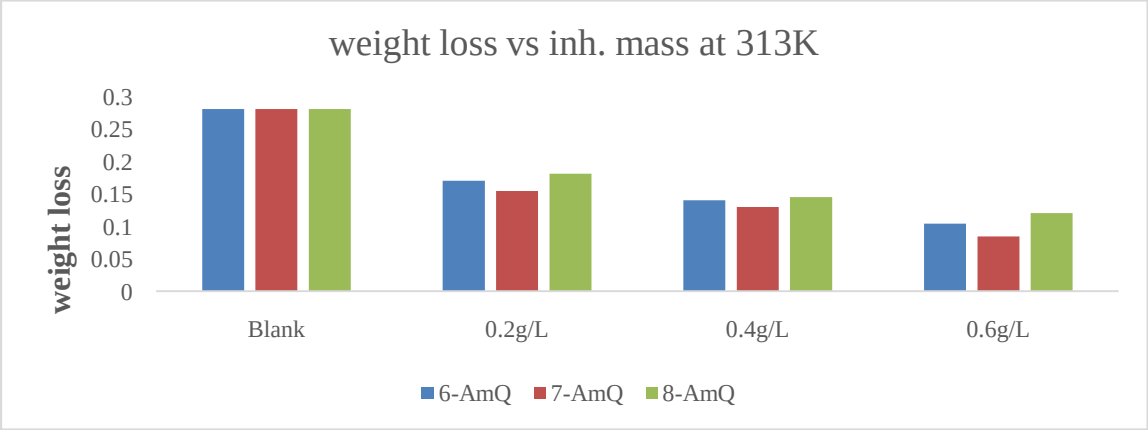

Figure 3.2: Weight loss of aluminium in 0.2M HCl at 313k using 6-AMQ, 7-AMQ and 8-AMQ inhibitors with varying mass for each system.

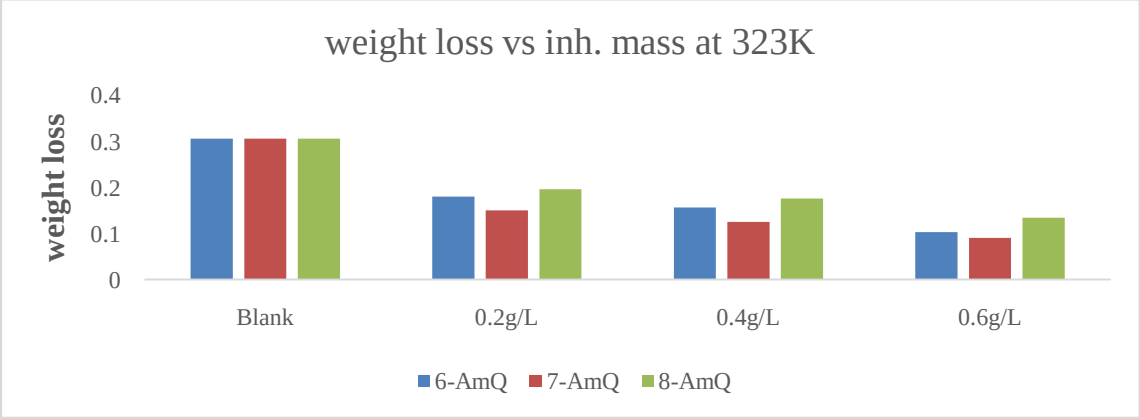

Figure 3.3: Weight loss of aluminium in 0.2M HCl at 323k using 6-AMQ, 7-AMQ and 8-AMQ inhibitors with varying mass for each system.

Also figure 3.1 to 3.3 gave a clear situation for the effect of varying temperature from 303K, 313K and to 323K. There's increase in weight loss of the metal as the temperature increases. This has been reported by many scholars [17]. It's because at elevated temperature the inhibitor molecules becomes segregated and more porous on the metal surface. This allows some contacts between the metal and the corrodent molecules hence more mass loss than the room temperature.

Another observable effect from all figures 3.1 to 3.3 is that 7-AMQ has the lowest weight loss (shortest bar) for all the inhibitor mass at all temperature. This is a clear indication that 7-AMQ is more adsorbed on the metal surface than the remaining inhibitors, and so regardless of the inhibitor dose applied, 7-AMQ exhibits relatively lower mass loss compared to 6-AQ and 8-AMQ, indicating clearly its superior anti-corrosion efficiency.

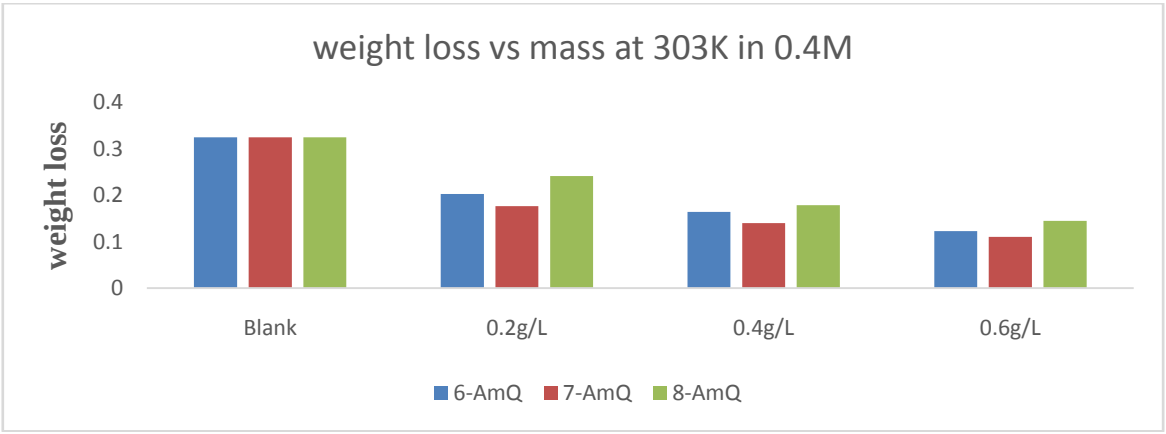

Figure 3.4: Weight loss of aluminium in 0.4M HCl at 303k using inhibitors 6-AMQ, 7-AMQ and 8-AMQ with varying mass for each system.

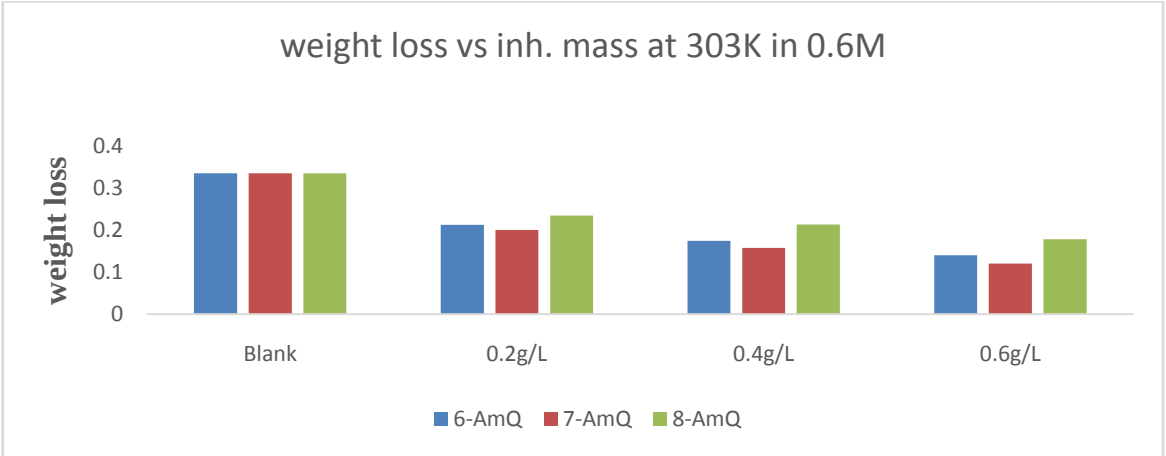

Figure 3.5: Weight loss of aluminium in 0.6M HCl at 303k using inhibitors 6-AMQ, 7-AMQ and 8-AMQ with varying mass for each system.

Figures 3.3 to 3.5 shows an increase in corrodent concentration with increase in mass loss of the metal serially irrespective of temperature and inhibitor mass. Corrosion was more rapid in 0.6M, followed by 0.4M and 0.2M has the lower corrosion of metal both in the absence and in the presence of inhibitor at all temperature . This may be attributed to the breakdown of the air-formed passive film and the initiation of pitting, which is traditionally followed by steady state corrosion conditions, due to cathodic reaction [18]. In most cases, the reason for varying the concentration of the corrodent in corrosion inhibition study is to allow study of how the adsorption behaviour changes with corrosiveness of the environment. it will also help to determine the optimal concentration of inhibitor for a given level of corrosion. As the concentration of the corrodent increases, the activation energy for the reaction decrease. This is because there are more corrodent molecules available to react, so they can provide more energy to overcome the energy barrier and start the reaction[19].

Figure 3.6: Corrosion Rate of aluminium in 0.4M HCl at 303k with varying inhibitor mass for each system.

3.2 Corrosion rate analysis

Corrosion rate is a measure of how quickly a material corrodes or goes into solution[19]. It can be expressed in terms of the amount of material lost over time, such as milligrams per square meter per day. Corrosion rate is an important factor to consider when studying corrosion inhibition, as the goal generally is to reduce the rate of corrosion[20]. The figures 3.6, 3.7 and 3.8 are the profile of the corrosion rate in 0.2MHCl at 303K, 313K and 323K respectively with varying inhibitor mass for each system. It can be observed from the above figures that increase in temperature also increases the corrosion rate generally for all the systems. However, the rate of attack slows down in the presence of inhibitors. As the concentration of the corrosion inhibitor increases, the corrosion rate tends to decrease[20]. This is because the inhibitor molecules adsorbed onto the metal surface forms a protective layer that prevents the metal from coming in contact with the corrosive environment [21]. The more inhibitor molecules there are, the thicker the protective layer and the slower the corrosion rate. All the figures 3.6, 3.7 and 3.8 indicates that the corrosion rate is slower with 7-AMQ as inhibitor being the inhibitor with shorter bar. 7-AMQ has been observed to be more attracted on the metal surface than other inhibitors used here. In this study, the corrosion rate is in the order 8-AMQ > 6-AMQ > 7-AMQ. The molecules have the same molecular mass and equal number of atoms, but there's noticeable difference in terms of performance in reduction of corrosion rate among them.

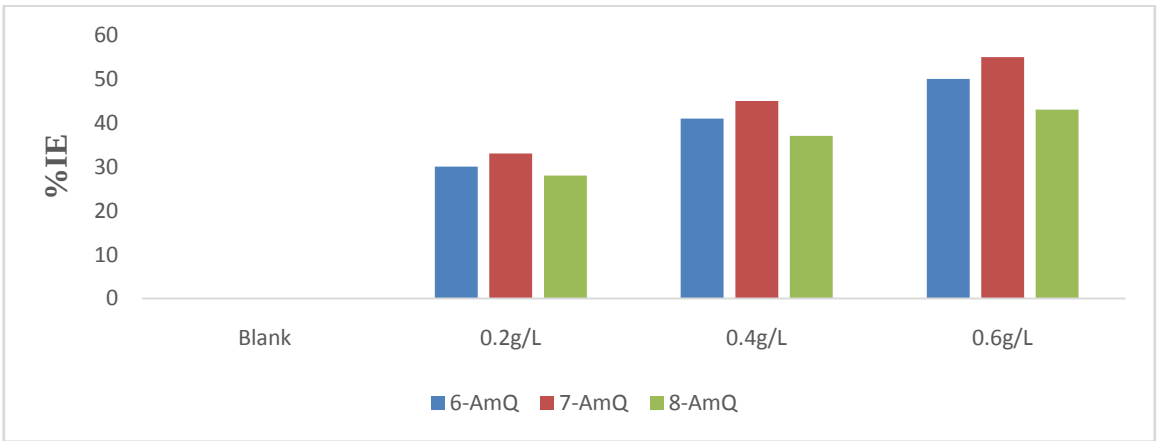

Figure 3.7: %IE for corrosion of aluminium in 0.2M HCl at 303k with varying inhibitor mass for each system.

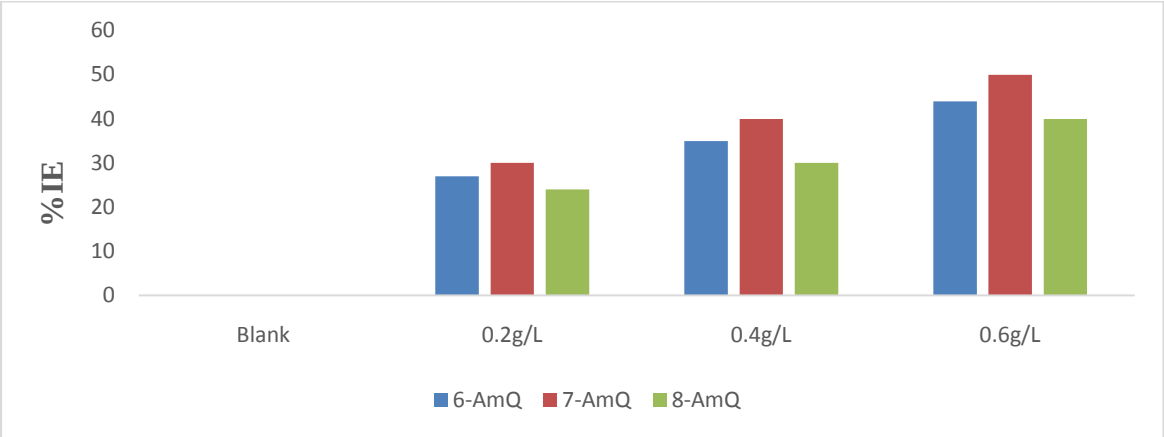

Figure 3.8: %IE for corrosion of aluminium in 0.2M HCl at 313k with varying inhibitor mass for each system.

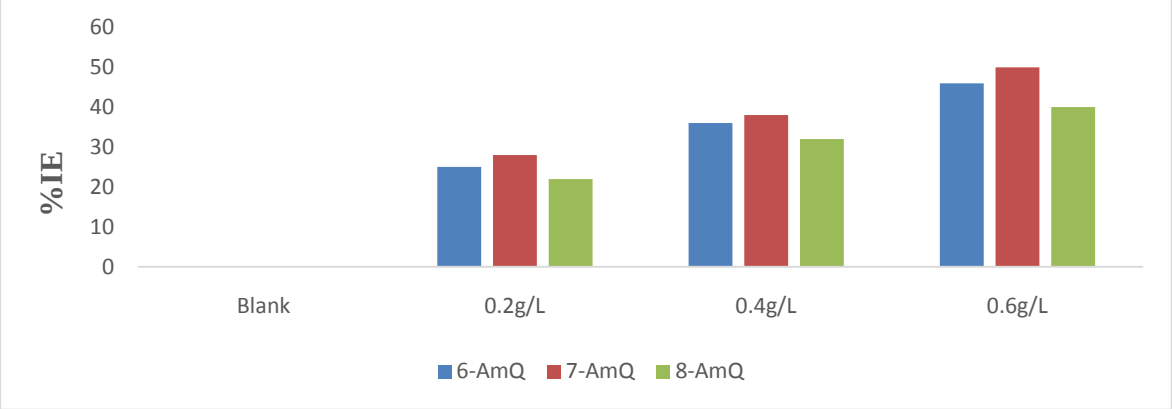

Figure 3.9: %IE for corrosion of aluminium in 0.2M HCl at 323k with varying inhibitor mass for each system.

The figures 3.7, 3.8 and 3.9 are the profiles of the percentage inhibition efficiency (%IE) in 0.2M HCl at 303K, 313K and 323K respectively with varying inhibitor mass for each system. Inhibition efficiency of a given inhibitor is the percentage reduction in corrosion rate when a corrosion inhibitor is added [21]. The above figures shows an increase in the vertical height of the bar with increase in the inhibitor mass for each of the inhibitor, which is the direct increase in the percentage inhibition efficiency as the mass of the inhibitor is increased at all temperatures. Also here unlike the weight loss and the corrosion rate, the percentage inhibition efficiency increased with increase in the inhibitor mass and decreased with elevation of temperature. Also here, despite the fact that the three molecules used here (6-AMQ, 7-AMQ and 8-AMQ) are comparably of the same molecular mass and number of atoms, but observably the molecule 7-AMQ has the highest percentage inhibition efficiency followed by 6-AMQ with 8-AMQ having the least. This can also be observed from table 3.1 which indicates the variation of inhibitor mass and temperature in 0.2M HCl. Both the values of the mass loss and the percentage inhibition efficiency are in consistent with the figures above. There are possible reasons for the difference in the corrosion rate and the percentage inhibition efficiencies among the three molecules which will be discuss after consideration of other experimental results (PDP and EIS) and the quantum chemical parameters here in.

Table 3.1 : Mass loss of the aluminium and the inhibition efficiency of each inhibitor with varying masses in 0.2M Hydrochloric Acid (Corrodent) at 303k, 313k and 323k

S/N	Inhibitor	Conc.g/L	Average mass loss (g) at 303k	%IE	Average mass loss (g) at 313k	%IE	Average mass loss (g) at 323k	%IE
	Blank	0	0.2110	0	0.2810	0	0.3061	0
1	6-AMQ	0.2	0.1206	47	0.15	32	0.1601	30
		0.4	0.0615	61	0.1102	48	0.1313	44
		0.6	0.0181	70	0.0701	53	0.1102	54
2	7-AMQ	0.2	0.1101	52	0.1343	48	0.1401	37
		0.4	0.0509	76	0.1002	59	0.1211	55

		0.6	0.0112	81	0.0501	73	0.0931	67
3	8-AMQ	0.2	0.125	33	0.1759	30	0.1836	26
		0.4	0.0740	55	0.1188	41	0.1635	37
		0.6	0.0412	62	0.0778	50	0.1121	46

The table 3.1 clearly shown the increase in mass loss with temperature increase, decrease in mass loss and increase in percentage inhibition efficiency with increase in inhibitor concentration which has also been reported by many authors [22]. From the observation of the parameters in the table, 7-AMQ has the better inhibitive performance follwed by 6-AMQ and 8-AMQ has the lowest performance under the same conditions. But generally all the molecules performances in terms of corrosion inhibition for aluminium in HCl environment are very good. The ultimate goal of using corrosion inhibitor is to prevent or minimized severe chemical attack on the metal surface to reasonable percentage which leads to economic and social consequences [22].

3.3 kinetic study

Table 3.2 : Kinetics for Corrosion of aluminium using 0.4g s of each inhibitor in 0.4M Hydrochloric Acid (Corrodent) at varying temperature.

Inhibitor	**6-AMQ**					
Temp.	303K		313K		323K	
	k_1	R^2	k_1	R^2	k_1	R^2
1st order	0.016	0.999	0.022	0.998	0.024	0.997
2nd order	0.001	0.542	0.004	0.239	0.005	0.498
Inhibitor7-AMQ						
Temp.	303K		313K		323K	
	k_1	R^2	k_1	R^2	k_1	R^2
1st order	0.018	0.999	0.024	0.999	0.026	0.999
2nd order	0.001	0.352	0.003	0.697	0.005	0.696
Inhibitor	**8-AMQ**					
Temp.	303K		313K		323K	
	k_1	R^2	k_1	R^2	k_1	R^2
1st order	0.014	0.997	0.020	0.998	0.022	0.999
2nd order	0.001	0.342	0.003	0.568	0.004	0.697

Tables 3.2 presented details of the kinetic parameters obtained from weight loss experiments for aluminium corrosion in HCl solutions using aminoquinolines at different temperatures. The value of the rate constant and the R-square value are the parameters for establishing the kinetics of chemical reaction at varying temperature [23]. In almost all systems, the R-square values are more close to unity for the first order results than that of the second order, and with higher values of the rate constant. This confirmed the fact that the corrosion inhibition of alumunium with aminoquinolines followed the first order kinetic. The first and the second order kinetic rate constant was obtained using equations 3.6 and 3.7 below:

$$-\frac{1}{t}\text{In}\frac{[A]}{[Ao]} = k_1(s^{-1}) \quad \text{or} \quad \frac{1}{t}\text{In}\frac{[Ao]}{[A]} = k_1 \qquad 3.6$$

$$\frac{1}{[A]} = k_2 t + \frac{1}{[Ao]} \qquad 3.7$$

Where $[A_o]$ is the initial mass of the metal, [A] is the mass corresponding to time t, k_1 and k_2 are the first and second order rate constant respectively [23].

3.4 Activation parameters

In order to calculate the values of activation energies and heat of adsorption, study of the effect of temperature on the corrosion of aluminium in varying HCl concentrations containing various masses of inhibitors is of paramount important and the following Arrhenius Equations werer used:

$$CR = Aexp\left(\frac{-Ea}{RT}\right) \qquad [24]. \qquad 3.8$$

Taking logarithm of both sides at a particular temperature gives Equation 3.9, while at two different temperatures gives Equation 3.10 as follows:

$$\log(CR) = \log A - \frac{Ea}{2.303RT} \qquad [24]. \quad . \qquad 3.9$$

$$\log\left(\frac{CR_2}{CR_1}\right) = \frac{Ea}{2.303R}\left(\frac{1}{T_1} - \frac{1}{T_2}\right) \qquad [24]. \quad . \qquad 3.10$$

$$Q_{ads} = 2.303R\left[log\left(\frac{\theta_2}{1-\theta_2}\right) - log\left(\frac{\theta_1}{1-\theta_1}\right)\right] x \frac{T_1 x T_2}{T_2 - T_1} kJ/mol \qquad 3.11$$

Where θ_1 and θ_2 are the degrees of surface coverage at the temperatures T_1 and T_2 respectively [24]. At constant pressure, the value of Q_{ads} approximate enthalpy of adsorption (ΔH_{ads}).
The free energy change of adsorption, ΔG^{o}_{ads}, is calculated using Equation 3.12 [25]:

$$\Delta G^{0}_{ads} = - RT \ln (55.5 \times K_{ads}) \quad 3.12$$

Where 55.5 is the molar concentration of water in solution, *R* and *T* remain the same as described above and K_{ads} was obtained from the intercept of a plot of θ against log*C*. For adsorption to take place, ΔG_{ads}must be negative. Now, ΔS_{ads} is always negative, because the adsorbed atoms or molecules lose degrees of freedom in the process. As a result, ΔH_{ads} also supposed to be negative showing that most of the adsorption processes are exothermic. Generally, the values of ΔG^{0}_{ads}around -20 kJmol^{-1} correspond to physisorption while those above -40 kJmol^{-1} correspond to chemisorption [26]. The heat of adsorption Q_{ads}, which can also be defined by equation 3.10 depends on the energies of the bonds formed between the adsorbed atoms and the metal surface[27].
The activation energy is the minimum energy required for the corrosion reaction to occur, while the heat of adsorption is the energy released when the inhibitor molecules are adsorbed on to the metal surface. The activation energy is related to the overall corrosion reaction, while the heat of adsorption is specific to the interaction between the inhibitor molecules and the metal surface[28].

Table 3.3: Activation Energy, E_a(kJ/mol) and Q_{ads} (kJ/mol) of Different Inhibitor Systems of 0.2, 0.4 and 0.6g/L on Aluminium at 313K and 323K Obtained through Weight Loss Method.

			6-AMQ(g/L)					
		0.00	0.2		0.4		0.6	
Corrodent concentration	Ea	Qads	Ea	Qads	Ea	Qads	Ea	Qads
0.2M	33.05	0.00	19.66	-34.28	13.54	-41.01	11.03	-87.01
0.4M	28.18	0.00	20.54	-28.69	16.08	-33.66	14.97	-80.17
0.6M	23.25	0.00	22.66	-27.27	19.24	-29.81	18.46	-67.09

			7-AMQ(g/L)					
		0.00	0.2		0.4		0.6	
Corrodent concentration	Ea	Qads	Ea	Qads	Ea	Qads	Ea	Qads
0.2M	33.05	0.00	12.98	-84.03	5.54	-93.99	4.17	-107.31
0.4M	28.18	0.00	17.29	-66.73	7.72	-78.35	5.31	-90.17
0.6M	23.25	0.00	19.61	-54.89	10.83	-63.63	7.78	-83.29

			8-AMQ(g/L)					
		0.00	0.2		0.4		0.6	
Corrodent concentration	Ea	Qads	Ea	Qads	Ea	Qads	Ea	Qads
0.2M	33.05	0.00	20.46	-27.86	18.31	-33.91	14.98	-65.69
0.4M	28.18	0.00	21.19	-23.66	17.21	-27.86	16.08	-57.22
0.6M	23.25	0.00	23.02	-19.64	21.16	-23.36	19.64	-33.68

The table 3.3 show a decrease in activation energy with increase in corrodent concentration without inhibitor. This is in consistent with the theory of chemical reaction, since collision of molecules that leads to chemical reaction. the gravity of this collision depends on the distance between the molecules [29]. When the concentration of the corrodent is increased, more molecules are introduce into the system and the distance between them is shortened hence less energy is required for activation of the reaction. So the higher the concentration of the corrodent, the lower will be the activation energy for the corrosion reaction.

The difference in activation energy and heat of adsorption with and without inhibitor suggest that the presence of the inhibitor is changing the mechanism of the corrosion [29]. Without inhibitor, the rate of corrosion is directly proportional to the concentration of the corrodent, and there is no heat of adsorption because the corrodent is not forming a bond with the metal surface. As shown in the table 3.3 with inhibitor, activation energy decreases as inhibitor mass increases, indicating that the inhibitor is lowering the barrier to the reaction and increasing the rate of corrosion. This could be due to the formation of a new bond between the inhibitor and the metal surface, which has a lower activation energy[30]. The increase in activation energy with increasing corrodent concentration when inhibitor is present suggest that the inhibitor is creating a barrier that make it harder for the corrodent to react with the metal surface. This could be due to formation of the layer of inhibitor molecules on the metal surface that blocks the corrodent from reaching the surface.

The increase in the heat of adsorption also suggests that a bond is being formed between the inhibitor and the metal surface[30]. Table 3.3 indicates that 7-AMQ has lower activation energy and higher heat of adsorption compared to the other molecules, followed by 6-AMQ and 8-AMQ has highest activation energy. This could be due to the unique structure of 7-AMQ which allows it to interact with the metal surface in a way that lowers the energy barrier for the reaction.

Table 3.4: Enthalpy, ΔH_{ads} (kJ/mol) and Entropy, ΔS_{ads} (kJ/mol/K) Values Obtained with and without Different Inhibitors Systems of 0.2, 0.4 and 0.6g/L on Aluminium through Weight Loss Method.

6-AMQ(g/L)								
Corrodent concentration	0.00 ΔH_{ads}	ΔS_{ads}	0.20 ΔH_{ads}	ΔS_{ads}	0.40 ΔH_{ads}	ΔS_{ads}	0.60 ΔH_{ads}	ΔS_{ads}
0.2M	32.92	0.197	25.95	0.212	22.55	0.227	17.88	0.235
0.4M	42.28	0.182	30.39	0.204	27.37	0.211	23.28	0.224
0.6M	51.77	0.167	40.55	0.187	38.48	0.199	29.87	0.207
7-AMQ(g/L)								
Corrodent concentration	0.00 ΔH_{ads}	ΔS_{ads}	0.20 ΔH_{ads}	ΔS_{ads}	0.40 ΔH_{ads}	ΔS_{ads}	0.60 ΔH_{ads}	ΔS_{ads}
0.2M	32.92	0.197	20.51	0.207	17.55	0.224	15.38	0.227
0.4M	42.28	0.182	25.82	0.201	21.63	0.201	18.32	0.215
0.6M	51.77	0.167	30.41	0.192	31.77	0.196	23.93	0.212
8-AMQ(g/L)								
Corrodent concentration	0.00 ΔH_{ads}	ΔS_{ads}	0.20 ΔH_{ads}	ΔS_{ads}	0.40 ΔH_{ads}	ΔS_{ads}	0.60 ΔH_{ads}	ΔS_{ads}
0.2M	32.92	0.197	25.97	0.213	23.55	0.228	19.89	0.231
0.4M	42.28	0.182	32.38	0.209	28.60	0.213	23.28	0.220
0.6M	51.77	0.167	43.60	0.189	39.47	0.198	30.87	0.211

From the table 3.4, the corrodent concentration increases, the enthalpy of the system increases which means that the system is becoming more energetically more favourable for the corrosion reaction to take place. This is because of the fact that the corrodent is the reactant in the corrosion reaction[31]. T he decrease in $\Delta S_{ad}$with increasing corrodent concentration also is an interesting issue, since the system is becoming more ordered as the corrodent molecules are added. However, the opposite trends are observed for the system with inhibitor mass. This suggest that the inhibitor is disturbing the corrosion reaction and making the system less energitic[31]. The $\Delta H_{ads}$and ΔS_{ad} values have opposite trends as the corrodent concentration increases. This is likely due to the fact that the inhibitor is having two different effects on the system. On the one hand it is blocking the corrosion reaction, which decreases the system's enthalpy. On the other hand it is increasing the disorder of the system, which increases the system's entropy. The net effect of these two opposing effects is observed in table 3.4 . This is a fascinating example of how two opposing forces can have a complex interaction to determine the overall properties of the system. The $\Delta H_{ads}$and ΔS_{ad} values for 7-AMQ has better precision than other two inhibitors. This is justifying the superiority of the 7-AMQ in terms of corrosion inhibition performance.

Generally, the inhibitors effects on the corrosion reaction can be summerized in two main points. First the inhibitor is blocking the reaction and preventing the loss of metal from the surface. Second, the inhibitor is increasing the disorder of the system, which may be helping to prevent the formation of corrosion products. The overall effect of inhibitor is to reduce the rate of corrosion reaction and to prevent the damage caused by corrosion[32]. This is very useful in practical applications where corrosion prevention is important.

The observations from table 3.4 reveal that the difference seen in the inhibition efficiencies in the table 3.1 does not emerged from the size of the substituent, but comes probably from the substituent position. In other word, the size of amino substituent attached to quinoline has no significant effect on the corrosion inhibition of aluminium in HCl solution. This reflects the characteristics of liquid or solid reactions likely to be aluminium dissolution due to ineffective inhibition [33].

Table 3.5: Langmuir Adsorption Isotherm Parameters Obtained from the Adsorption of the Inhibitors on Aluminium Surfaces at Different Temperatures.

		303K			313K			323K		
Inhibitor	Corr. Conc.	R^2	Slope	K_{ads}	R^2	Slope	K_{ads}	R^2	Slope	K_{ads}
6-AMQ	0.2MHCl	0.999	0.323	1.371	0.987	0.571	0.825	0.998	0.628	0.688
	0.4MHCl	0.996	0.403	0.830	0.997	0.412	0.777	0.984	0.459	0.683
	0.6MHCl	0.994	0.455	0.713	0.899	0.479	0.697	0.994	0.498	0.550

		303K			313K			323K		
Inhibitor	Corr.Conc.	R^2	Slope	K_{ads}	R^2	Slope	K_{ads}	R^2	Slope	K_{ads}
7-AMQ	0.2M HCl	0.998	0.329	0.941	0.999	0.655	0.644	0.992	0.631	0.625
	0.4M HCl	0.846	0.490	0.692	0.995	0.529	0.646	0.878	0.463	0.639
	0.6M HCl	0.972	0.315	0.833	0.996	0.510	0.599	0.997	0.636	0.428

		303K			313K			323K		
Inhibitor	Corr.Conc.	R^2	Slope	K_{ads}	R^2	Slope	K_{ads}	R^2	Slope	K_{ads}
8-AMQ	0.2MHCl	0.997	0.414	0.869	0.999	0.592	0.620	0.997	0.666	0.517
	0.4MHCl	0.913	0.561	0.584	0.921	0.626	0.506	0.958	0.628	0.459
	0.6MHCl	0.990	0.313	0.791	0.989	0.527	0.515	1.000	0.517	0.435

3.5 Adsorption Study

The adsorption isotherms provide valuable information on the nature of interaction between the inhibitor molecules and the metal surface. The surface coverage (θ) of the adsorbed molecules can be determined by dividing the inhibition efficiency values of the weight loss runs with 100 [34]. The results obtained for θ were analyzed using Langmuir, Temkin, Flory Huggins and El-Awardy adsorption isotherm equations as given by equations 3.13, 3.14, 3.15 and 3.16 respectively.

$$\frac{C}{\theta} = \frac{1}{K} + C \qquad 3.13$$

$$\theta = \frac{-\ln\log K_{ads}}{2\alpha} - \frac{\ln C}{2\alpha} \qquad 3.14$$

$$\log\frac{(\theta)}{C} = \log K + x\log(1-\theta) \qquad 3.15$$

$$\log\frac{\theta}{(1-C)} = \log K + y\log C \qquad 3.16$$

where*C* is the concentration of the inhibitor in g/L and K_{ads} is the equilibrium constant of the adsorption process. The Langmuir adsorption isotherm parameters are shown in Table 3.5 The linear regression coefficient is close to unity for almost all the inhibitors. The degrees of surface coverage, θ, at various concentrations of the selected quinolines at 303 and 323 K were the data used for plotting the isotherms. The data were tested with the different adsorption isotherm equations viz Langmuir, Temkin, Flory-Huggins and El-Awady show the parameters of linearisation of each adsorption model[35].

The surface coverage obtained from IE% values fitted all the adsorption models since the values of the regression coefficient, R^2 , were mostly greater close to unity in Langmuir for all the three systems [35]. But the Langmuir adsorption isotherm fited the best with almost all the systems have R^2 values close to unity. Sometimes, it may be sufficient to confirm inhibitor adsorption from data which fit the isotherms. Often times, it is also desirable to extend the scope to include deduction of thermodynamic parameters associated with the adsorption process using the relationship between the adsorption equilibrium constant (kads) and the standard free energy of adsorption, ΔGads[36].

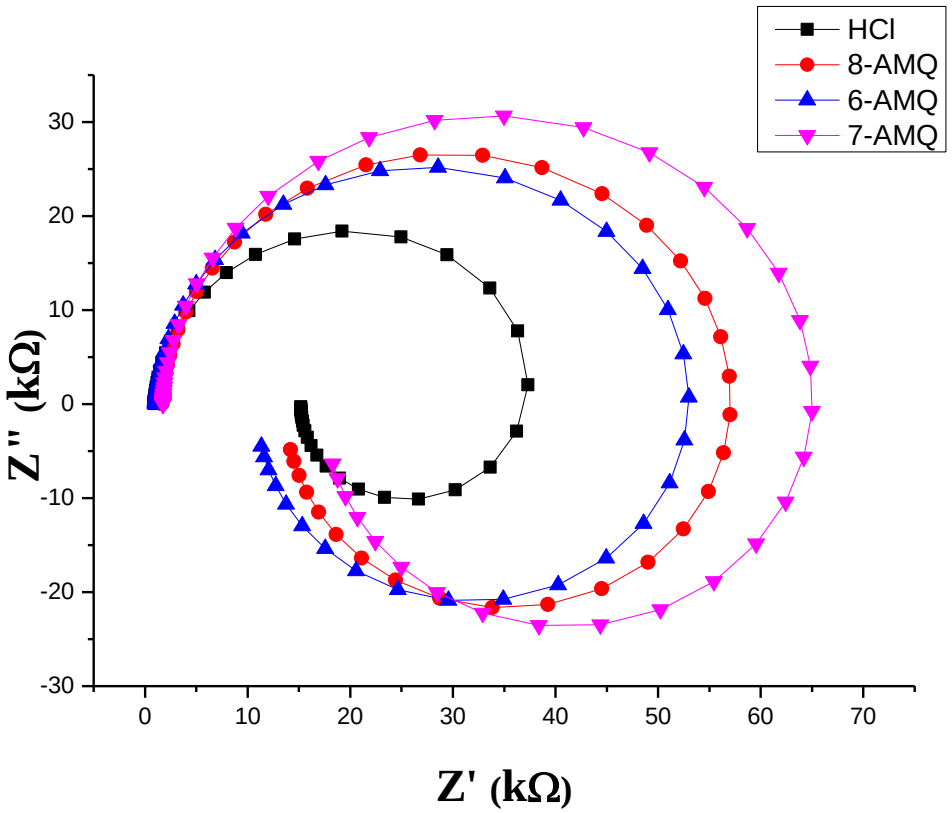

Figure 4.10: Impedence responses at the metal/acid interface for the corrosion of aluminiumin the absence and in the presence of 0.4g/L 6-AMQ, 7-AMQ and 8-AMQ inhibitors in 0.4M HCl at 303k.

The figure 3.10 depict the characteristics impedance responses at the metal/acid interface fors the corrosion of aluminium in the absence and in the presence of 0.4g/L each inhibitor in 0.4M HCl. The impedance spectra for the Nyquist plots of aluminium in the acid solutions in the absence and presence of the aminoquinolines were appropriately analyzed by fitting to the equivalent circuit model Rs (C_{dl} ,Rct), which has been previously used to model the metal/acid interface[35], [36].

Table 3.6 : Impedance data for the corrosion of aluminium in 0.4 M HCl in the absence and presence of 0.4g/L Inhibitor for each system at 303 K.

System	R_{ct} (Ω cm^2)	C_{dl} ($\mu\Omega^{-1}S^n cm^{-2}$)	N	IE%	
HCl (Blank)	134.53.56	0.86	0.00		
6-AMQ	179.5	2.31	0.84	49.92	
7-AMQ	237.2	2.01	0.85	54.34	
8-AMQ	156.4	2.52	0.86	35.08	

The corresponding impedance parameters are presented on Table 3.6. The increase in Rct values in inhibited systems which signifies an increase in the diameters of the Nyquist semicircles with a corresponding decrease in the double layer capacitance (C_{dl}), confirms the corrosion inhibiting properties of the quinolines . The observed decrease in C_{dl} values, which normally corresponds to alteration of the double layer thickness can be attributed to the adsorption of the quinolines (with lower dielectric constant compared to the displaced adsorbed water molecules) on the metal/acid interface, thereby protecting the metal from the corrosive effect of the aggressive acids. However, 7-AMQ has largest amplitude among the three aminoquinolines tested as observed from figure 3.10 and highest percentage inhibition efficiency as shown on table 3.6 which further justified its corrosion inhibition superiority compared to 6-AMQ and 8-AMQ. The amplitude of the Nyquist plots, the magnitude and trend of the obtained inhibition efficiencies %IE presented are in agreement with those determined from weight loss measurements.

[

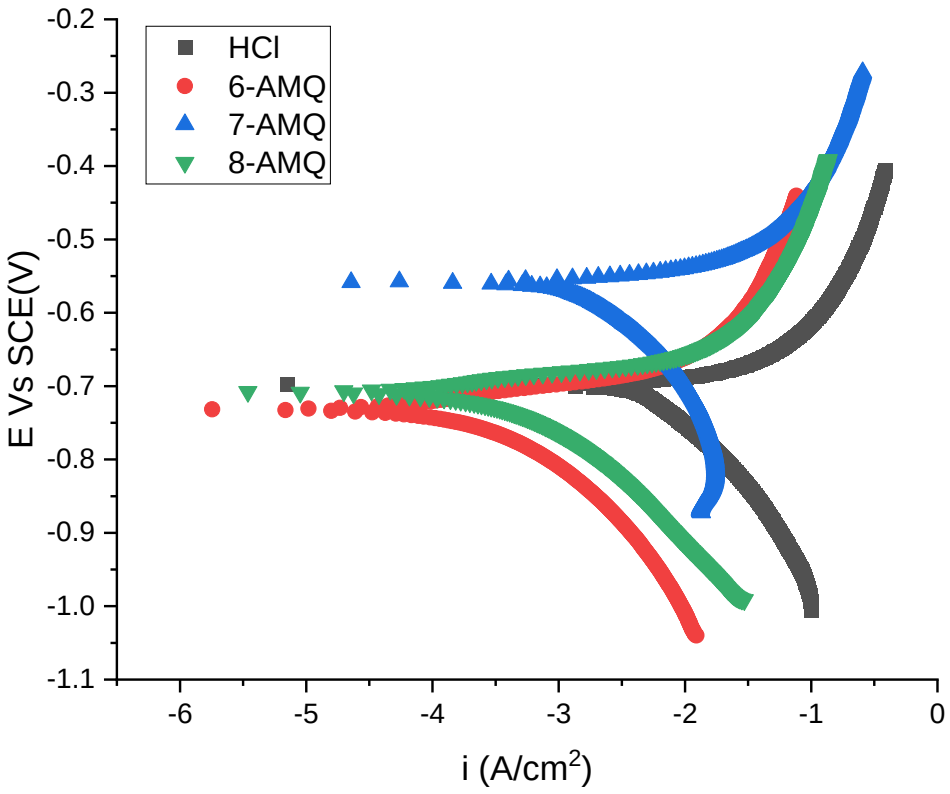

Figure 4.11: Polarization at the metal/acid interface for the corrosion of aluminium in the absence and in the presence of 0.4g/L 6-AMQ, 7-AMQ and 8-AMQ inhibitors in 0.4M HCl at 303k**.**

From Table 3.7, it can be clearly seen that, the insertion of aluminium in the corrodent (HCl) of 0.4M concentration without inhibitor gives higher value of both the i_{corr} and the corrosion rate at room temperature, but they tend to decrease as the inhibitors are introduce in the corrosive solution, which in turn leads to some degrees if inhibition. For the first system with 6-AMQ (6-aminoquinoline) of 0.4g/L, lower the i_{corr} value of 17.20µA to 600.00 µA was obtained, while the corrosion rate and inhibition efficiency achieved were 385mpy and 42.16% respectively.

The potentiodynamic polarization plots show that the inhibitor affects both the anodic metal dissolution and cathodic hydrogen evolution reactions [37]. In some of the inhibitors used, the cathodicTafel lines are parallel for all the inhibitors, which indicates that the inhibitor molecules just slightly change the cathodic hydrogen evolution reaction.

Table 3.7 :Potentiodynamic polarization data for the corrosion of aluminium in 0.4 M HCl in the absence and presence of 0.4g/L Inhibitor for each system at 303 K.

System	BetaA(V/d)	BetaC(V/d)	i_{corr}(µA)	E_{corr}(mV)	CR (mpy)	%IE
Blank	188.2e-3	414.2e-3	617.20	-998.0	11.02e3	0.00
6-AMQ	1.275	271.0e6	27.00	-699.00	5.9e3	40.32
7-AMQ	156.2e-3	179.4e-3	6.160	-659.00	3.957e3	64.04
8-AMQ	3.193	10.98	998.00	-704.00	8.5e3	34.46

The corrosion potential (E_{corr}) values from Table 3.7 show that the addition of inhibitor shifts the corrosion potential to positive side. When the corrosion potential changes noticeably with the introduction of an inhibitor, the inhibitor is claimed to work by blocking the active sites [37]. On the other hand, a negligible change in E_{corr} upon the addition of an inhibitor indicates that the inhibitor works by geometric blocking effect [37]. Hence, in these systems, the inhibitors are believed to work by blocking the active sites. Also from Table 3.7, it is observed that the I_{corr} value decreases with inhibitor addition, whereas the E_{corr} increases. Such a trend

of increase in E_{corr} accompanied with a drop in I_{corr} is suggestive of corrosion inhibition and increased surface hydrophobicity, which could be attributed to the inhibitor molecules adsorbed on aluminium surface [38]. In the present study, the largest shift caused in the E_{corr} upon inhibitors addition are mostly 40 mV and less, and both cathodic and anodic processes are affected, indicating that the inhibitors surely works as mixed type [38].

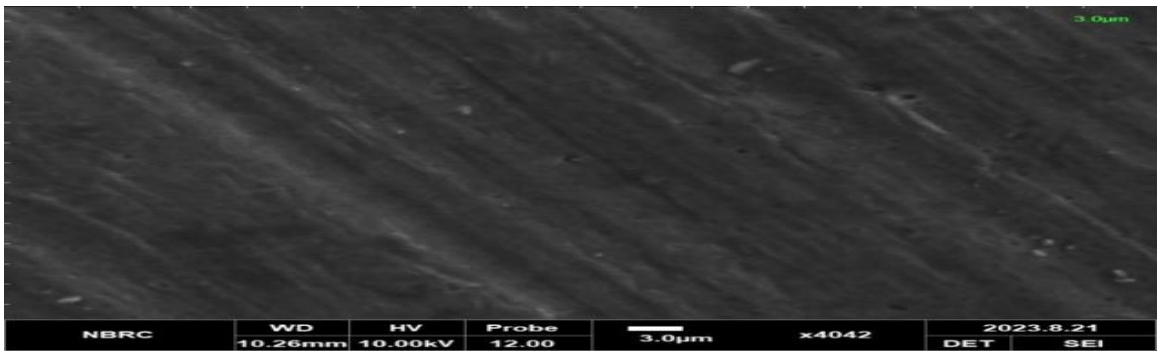

Figure 3.12: Micrograph of the Raw Aluminium image prior to corrosion study.

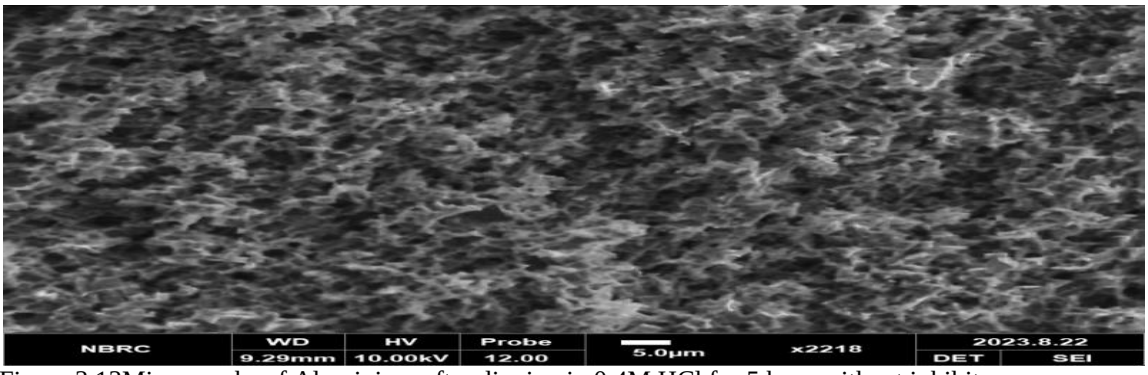

Figure 3.13Micrographs of Aluminium after dipping in 0.4M HCl for 5 hour without inhibitor.

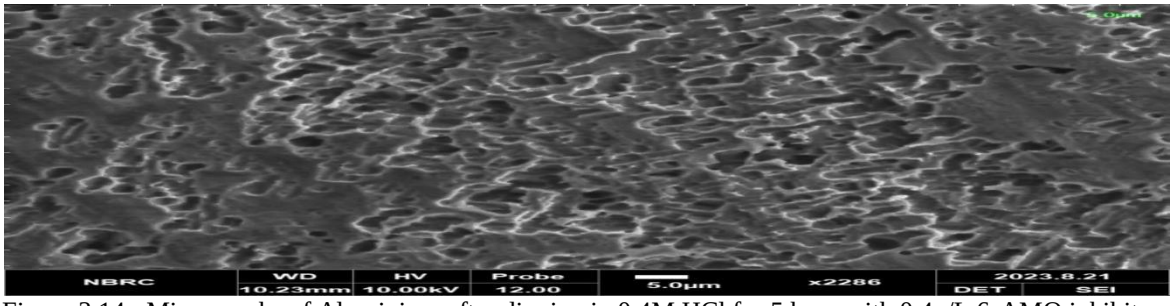

Figure 3.14 : Micrographs of Aluminium after dipping in 0.4M HCl for 5 hour with 0.4g/L 6-AMQ inhibitor.

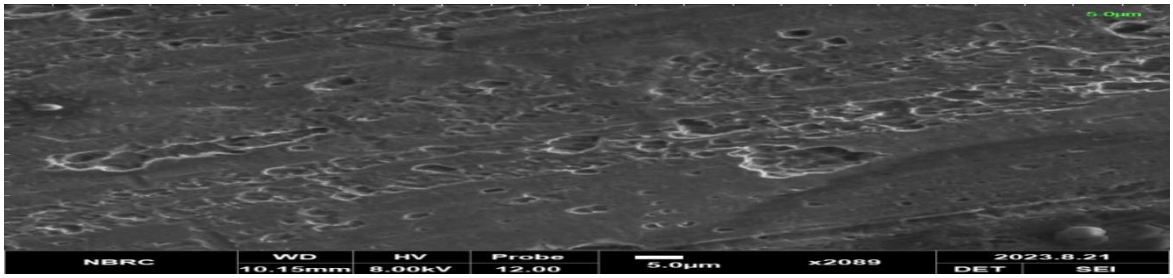

Figure 3.15 : Micrographs of Aluminium after dipping in 0.4M HCl for 5 hour with 0.4g/L 7-AMQ inhibitor.

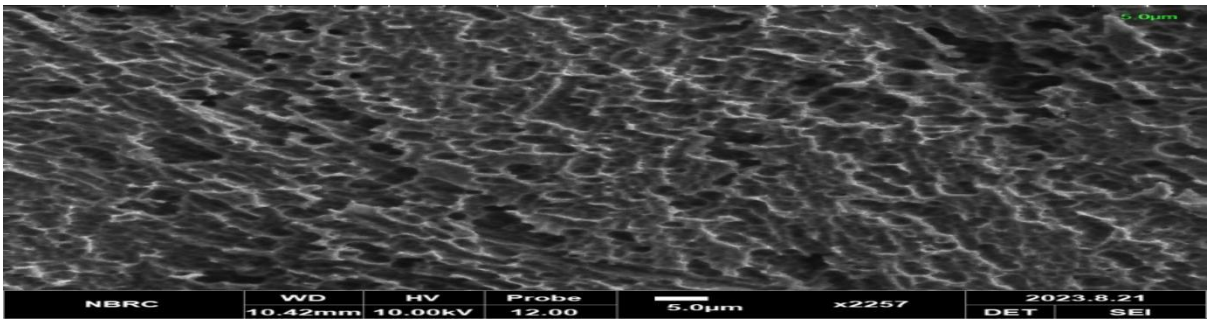

Figure 3.16 : Micrographs of Aluminium after dipping in 0.4M HCl for 5 hour with 0.4g/L 8-AMQ inhibitor.

Figure 3.12 shows the morphology of the aluminium surface prior to corrosion study, which indicates a smooth and clear surface. Figure 3.13 is the micrograph of the same surface after been immersed in 0.4M HCl solution without the inhibitor. Corrosion pits are clearly observed on the surface after 5 hours of immersion, which indicates the effects of the aggressive environment[39].

Figures 3.14,3.15 and 3.16 shows the micrographs of each of the samples immersed in 0.4M with 6-AMQ, 7-AMQ and 8-AMQ inhibitors respectively. It is clearly seen that the samples immersed in medium with inhibitors each shows a thick layer,which would have been formed from deposition of corrosion products and inhibitor molecules. The unprotected sample shows formation of more pits. The surface becomes hydrophobic with the addition of an inhibitor, which also confirms adsorption of the quinolinederrivatives molecules on the surface of the aluminium and formation of film to protect the surface, which is typical for mixed inhibitors [39]. However, figure 3.15 which is the surface using 7-AMQ inhibitor, shows more uniform layer on the aluminium protected surface which means more corrosion protection than 6-AMQ and 8-AMQ inhibitors. This is in consistent with the weight loss and the electrochemical experiments.

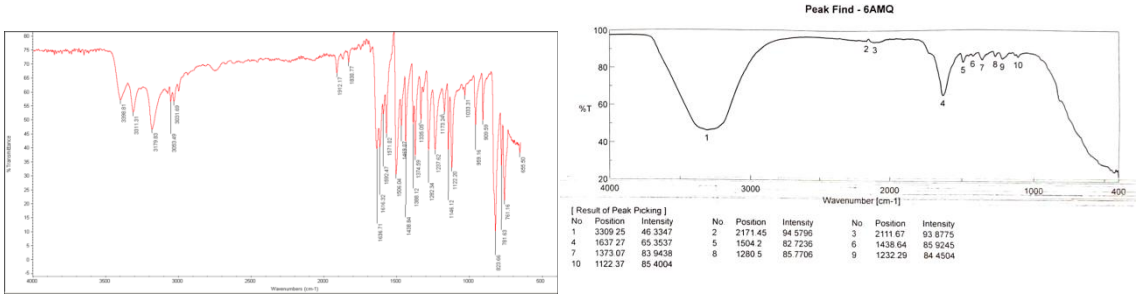

Figure 3.17 :FTIR spectra of Aluminium corrosion products after immersion in 0.4MHCl with and without 0.4g/L 6-AMQ at 303K

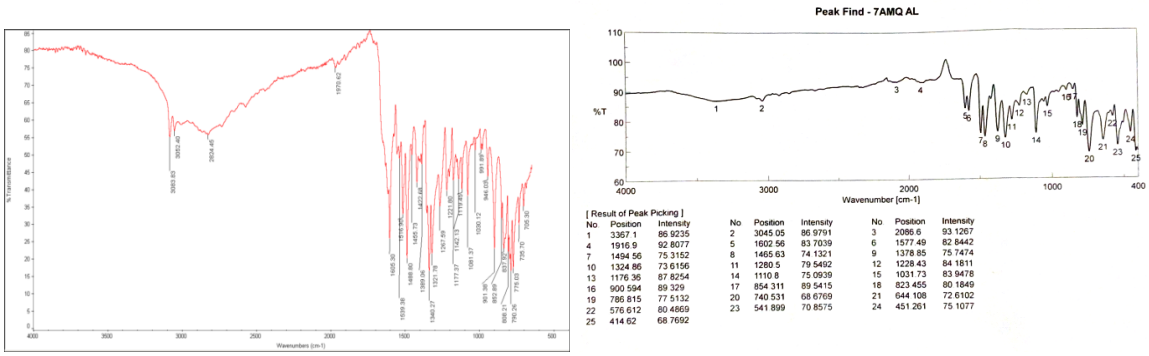

Figure 3.18 :FTIR spectra of Aluminium corrosion products after immersion in 0.4MHCl with and without 0.4g/L 7-AMQ at 303K

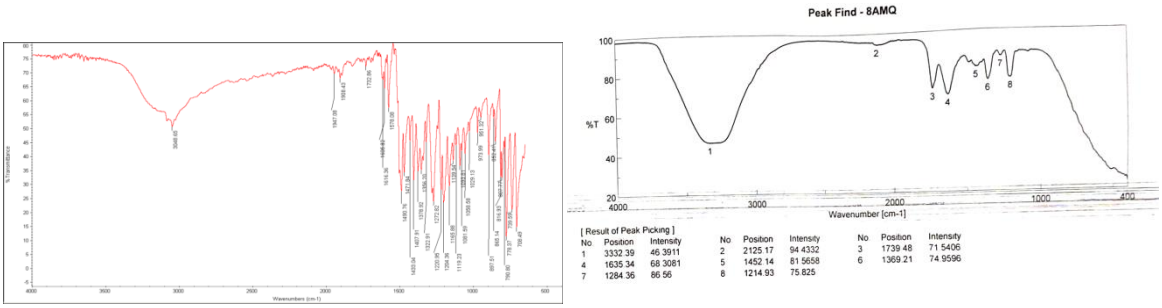

Figure 3.19 :FTIR spectra of Aluminium corrosion products after immersion in 0.4MHCl with and without 0.4g/L 8-AMQ at 303K

3.6 Fourier Transform IR Analysis

The FTIR spectra of the methylquinolinesderivatives on the surface of aluminium is shown in figure 3.17, 3.18 and 3.19 for 6-AMQ, 7-AMQ and 8-AMQ respectively. The 0.4g/L of the aminoquinolines in 0.4MHCl without insertion of the aluminium coupon shows clear the presence of amino group, aromatic ring, nitrogen and carbon-carbon double bond in the FTIR specra. The appearance of a strong peak around 3475cm^{-1}, 3505cm^{-1} and 3487cm^{-1}are due to the amino group (N-H) in 6-AMQ, 7-AMQ and 8-AMQ respectively, the peak around 1610cm^{-1} corresponds to the aromatic ring, the nitrogen atom in the molecule have a peak around 1410cm^{-1}, the peak around 1597cm^{-1} stands for the carbon-carbon double bond (C=C) and the peak at 1595cm^{-1} is assigned to carbon-nitrogen stretching vibration generally for all the aminoquinoline molecules. However, upon insertion of the aluminium in the solution, a new peak appears at 465cm^{-1} which indicates nitrogen-metal bond. The peak corresponding to amino group stretching at 3475cm^{-1} slightly shifted to 348545cm^{-1} for 6-AMQ, 3505cm^{-1} shifted to 3515cm^{-1} 7-7AMQ and 3487cm^{-1} shifted to 3495 for 8-AMQ molecule. The aromatic ring at 1615cm^{-1} changes to 1513cm^{-1}, peak of nitrogen which appears around 1410cm^{-1} shifted to 1420cm^{-1} in 6-AMQ and 8-AMQ, but has disappeared in 7-AMQ molecule. From the FTIR, Such a shift is attributed to the interaction of the aminoquinoline molecules with the metal surface [39]. A major interesting thing to consider is the effect of the substituent position on the FTIR spectrum. The positions of amino group on carbon atom number 7 (7-aminoquinoline) is orthor position relative to the nitrogen atom, so is more close to the region of high electron density around the nitrogen than in the meta or para position (6-aminoquinoline or 8-aminoquinoline) this makes 7-aminoquinoline more adsorbed on the metal surface. This electronic effect is known as mesomeric effect, which affect its FTIR spectra .The high stretching value of the amino peak and the disappearance of the peak of N after contact with the aluminium which is observed with 7-AMQ has also further justified its superior corrosion inhibition over the other molecules (6-aminoquinoline and 8-aminoquinoline) of the same molecular weight, this is an evidence of bonding with aluminium surface with the aminoquinoline molecules. This reaffirmed the fact that the mechanism proceeded via both physical and chemical adsorption[40].

3.7 Mechanism of Inhibition

Naturally, the test aluminium plate before corrosion study have air passive film of aluminium oxides on their surface due to oxidation as shown in equation (3.17).

$$4Al + nH_2O + 3O_2 \rightarrow 2Al_2O_3(H_2O)n \qquad 3.17$$

However, the dissolution of the aluminium in the aggressive medium (acid solution) can be represented in equation (3.18) [41]

$$Al \rightarrow Al^{3+} + 3^{e-} \qquad 3.18$$

The quinoline derivatives used here are the 6-AMQ, 7-AMQ and 8-AMQ are of the same molecular mass and similar structure. The interaction of aluminium with these molecules generally involves formation of complex between the aluminium ion, the double bond of the ring and nitrogen atoms of the aminoquinoline molecules. The complex is hydrophobic and act as corrosion inhibitor by blocking the active sites on the aluminium surface, thus preventing the reaction between the aluminium and the corrosive medium. The most likely chemical equation for this interaction is presented in the equation (3.19)

$$Al^{3+} + 3C_9H_9N_2 + 6H_2O \rightarrow [Al(C_9H_9N_2)_3]^{3+} + (H_2O)_3 \qquad 3.19$$

Here the aluminium ion (Al^{3+}) is complexed with three molecules of the aminoquinoline and six molecules of water forming a product that is hydrophobic. The interaction involves the formation of a coordinate covalent bond between the aluminium ion and the amino group of the aminoquinolinemolecule[41]. Furthermore, from the FTIR peak, the difference in the inhibition efficiency shown by the molecules despite having the same mass and structure is believed to come from orientation of the substituent (amino group) position on the parent

quinoline molecule. At position 7 , nitrogen is more available to participate in the interaction with the aluminium than other positions 6 and 8. This gives the superior performance for 7-AMQ.

IV. Conclusion

The influence of amino substituent position on quinoline used as corrosion inhibitor for aluminium in hydrochloric acid was successfully investigated experimentally. Out of the three aminoquinoline derivatives (6-aminoquinoline, 7-aminoquinoline and 8-aminoquinoline), 7-aminoquinoline showed highest corrosion inhibition efficiency under all conditions. The results obtained from mass loss, potentiodynamic polarisation and impedance measurement supported these observations. The position of the amino substituent group on the quinoline molecule showed some influence in the corrosion inhibition performance for the aluminium in acidic environment. Scanning electron micrographs confirmed that 7-AMQ has more uniform blockage of the etching sites on the acid-stricken aluminium slabs.Based on this, we can say that 7-AMQ is an effective corrosion inhibitor because it forms a stronger bond with the metal surface and lowers the activation energy for the corrosion reaction. This suggest that 7-AMQ is a promising candidate for use in industrial applications where corrosion prevention is in need. From the FTIR spectra, the significant shift in wave-number is attributed to the interaction of the aminoquinoline molecules with the metal surface. The high stretching value of the amino group peak and the disappearance of the peak of N which is seen with 7-AMQ, is an evidence of bonding of aluminium surface with the aminoquinoline molecules. This reaffirmed that the mechanism proceeded via mixed adsorption. The position of amino group on carbon atom number 7 (7-aminoquinoline) is orthor position relative to the nitrogen atom, so is more close to the region of high electron density around the nitrogen than in the meta or para position (6-aminoquinoline or 8-aminoquinoline) this makes 7-aminoquinoline more adsorbed on the metal surface hence justified its corrosion inhibition superiority over 6 and 8-aminoquinolines despite having the same molecular mass.

References

[1]. Abdallah M.(2002) " Rhodanineazosulpha drugs as corrosion inhibitors for corrosion of 304 stainless steel in hydrochloric acid solution, Journal of Corrosion Science; Vol. 44: 717–728.

[2]. Ali G. Sayed, Ashraf M. Ashmawy and M.A. Deyab (2023) "Synthesis , description and application of novel corrosion inhibitors for CS AISI1095 in 1.0MHCl based on benzoquinoline derivatives, Scientific Reports, Vol. 13 (13761)

[3]. Awad, M.K. (2004). Semiempirical investigation of the inhibition efficiency of thiourea derivatives as corrosion inhibitors Journal of elctroanalytical chemistry,567: 219– 225.

[4]. Babic´-Samardz˘ija, K. and Hackerman, N. (2006). Iron corrosion inhibition with dihydrobis - and hydrotris-(1-pyrazolyl)borates. Anti-corrosion Method and Material,53 : 19– 29.

[5]. Babic´-Samardz˘ija, K.,Khaled, K.F. and Hackerman, N. (2005a). Investigation of the inhibiting action of O-, S- and N-dithiocarbamato(1,4,8,11- tetraazacyclotetradecane)cobalt(III) complexes on the corrosion of iron in HClO 4 acid Applied Surface Science 240 : 327–340.

[6]. Chi, M. and Zhao, Y.P. (2009). Adsorption of formaldehyde molecule on the intrinsic and Al-doped grapheme: A first principle study. Computional Materials Science, 48:1085–1090.

[7]. Cicek V. and B. Al-Numan(2011), "Corrosion Chemistry. United States of America: Scrivener Publishing LLC & Wiley & Sons, 2011, pp. 7–14.

[8]. Dai W., and Zhang, Y.Y. (2012). Molecular dynamics simulation of the adsorption behaviour of amino acid corrosion inhibitor on Cu (1 0 0) surface. Applied Mechanics and Materials, 121-126: 226-230.

[9]. Dai, W. and Zhang, Y.Y. (2012). Molecular dynamics simulation of the adsorption behaviour of amino acid corrosion inhibitor on Cu (1 0 0) surface. Applied Mechanics and Materials, 121-126: 226-230.

[10]. Dakeshwar Kumar Verma, Ruby Aslam, JeenatAslam and Mumtaz Ahmad Quraishi (2021) "CmputationalModeling: Theoretical Predictive Tools for Designing of Potential Organic Corrosion Inhibitors, Journal of Molecular Structure, Vol. 1236:130294

[11]. Eddy, N.O., Odoemelam, S.A. andOdiongenyi, A.O. (2009). Inhibitive, adsorption and synergistic studies on ethanol extract of Gnetumafricana as green corrosion inhibitor for mild steel in H2SO4. Green Chemistry Letters and Reviews,2(2): 111-119.

[12]. EI-Awady, A.A., Abd-EI-Nabey, B.A. and Aziz, S.G. (1992). Kinetic-thermodynamic and adsorption isotherms analyses for the inhibition of the acid corrosion of steel by cyclic and open-chain amines. Journal of the Electrochemical Society, 139(8):2149-2154.

[13]. Ekanem, U.F., Umoren, S.A., Udousoro I.I. and Udoh, A.P. (2010). Inhibition of mild steel corrosion in HCl using pineapple leaves (Ananascomosus L.) extract. Journal of Materials Science. 45(20): 5558-5566.

[14]. Elfaydy M., Lgaz H., Salghi R., Larouj M., Jodeh S., Rbaa M., Oudda H., Toumiat K. and Lakhrissi B. (2016) " Investigation of corrosion inhibition mechanism of quiniline Derivative on Mild steel in 1.0M HCl Solution : Experimental, Theoretical and Monte Carlo simulation, Journal of material and Environmental Science. Vol. 7(9) 3193-3210, ISSN: 2028-25086.

[15]. El-HassanAssiriMajidDriouch, JamilaLazrakZakariae, BensoudaAliElhalouiandMouhcineSfaira (2020) " Development and validation of QSPR models for corrosion inhibition of carbon steel by some pyridazine derivatives in acidic medium, Heliyon, Vol.15, 50-67

[16]. Enenebeaku, C.K. (2011). Electrochemical studies of the inhibitory effects of selected plant extracts on the acid corrosion of mild steel. Ph.D Thesis. Federal University of Technology, Owerri.

[17]. Erazua E.A. and Adeleke B.B. (2019) "A Computational Study of Quinoline Derivatives as Corrosion Inhibitors for Mild Steel in Acidic Medium, Journal of Applied Science and Environmental Management, Vol. 23 (10) 1819-1824

[18]. Ezeoke AU, Adeyemi OG and Akerele OA (2012) "Computational and experimental studies of 4-Aminoantipyrine as corrosion inhibitor for mild steel in sulphuric acid solution. Int J Electrochem Sci.;7:534.

[19]. Fragoza-Mar L., O. Olivares-Xometl, M. A. Domínguez-Aguilar, E. A. Flores, P. Arellanes- Lozada, and F. Jiménez-Cruz (2012), "Corrosion inhibitor activity of 1,3-diketone malonates for mild steel in aqueous hydrochloric acid solution," Corrosion Science, vol. 61, pp. 171–184.

[20]. Gasparac, R., Martin, C.R., Stupnisek-Lisac, E. and Mandic, Zoran. (2000b). In situ and ex situ studies of imidazole and its derivatives as copper corrosion inhibitors II. AC Impedance, XPS, and SIMS Studies. Journal of the Electrochemical Society, 147(3): 991-998.

[21]. Hamadi L., S. Mansouri, K. Oulmi, and A. Kereche (2018) "The use of amino acids as corrosion inhibitors for metals: A review," Egyptian Journal of Petroleum, vol. 27, no. 4, pp. 1157–1165.

[22]. KadapparambilSumithra, KavitaYadav, ManivannanRamachandran and Noyel Victoria Selvam (2017) "Electrochemical investigation of the corrosion inhibition mechanism of Tectonagrandis leaf extract for SS304 stainless steel in hydrochloric acid, De Gruyter,DOI 10.1515/corrrev-2016-0074

[23]. Khaled K.F. and N. S. Abdel-Shafi (2011) "Quantitative Structure and Activity Relationship Modeling Study of Corrosion Inhibitors: Genetic Function Approximation and Molecular Dynamics Simulation Methods, International Journal Of Electrochemical Science, Vol.6 4077 - 4094

[24]. Kiani M. A. Mousavi, M. F., Ghasemi, S. Shamsipur, M. and Kazemi, S. H. (2008). Inhibitory effect of some amino acids on corrosion of Pb–Ca–Sn alloy in sulphuric acid solution.Corrosion Science 50: 1035–1045.

[25]. Moussa M N, Fouda A S, Taha F I and Eluenna A. (1988) "Comparative studies of aluminium corrosion in HCl medium using organic inhibitor, Bull Korean Chemical Society, 9(4) 191.

[26]. Olufunmilayo O. Joseph and Olakunle O. Joseph (2020) "Corrosion Inhibition of Aluminium Alloy by Chemical Inhibitors: An Overview, IOP Conference Series: Materials Science and Engineering, Volume 1107

[27]. R.K. Roy, S. Pal, K. Hirao, (1999) On non-negativity of Fukui function indices, J. Chem. Phys. 110 8236e8245, https://doi.org/10.1063/1.478792.

[28]. Shehu U. Najib, U. I. Gaya and Muhammad A. A. (2019) 'Influence of Side Chain on the Inhibition of Aluminium Corrosion in HCl by α-Amino Acids, King Mongkut's University of Technology North Bangkok.

[29]. Singh P, Ebenso EE and Olasunkanmi LO (2016) "Electrochemical, theoretical, andsurface morphological studies of corrosion inhibition effect of green naphthyridine derivatives on mild steel in HCl. J Phys Chem.;120(6):3408. DOI: https://doi.org/10.1021/acs.jpcc.5b11901

[30]. Soltani N., Tavakkoli, M. Khayatkashani, and M. R. Jalali(2012), "Green approach to corrosion inhibition of 304 stainless steel in hydrochloric acid solution by the extract of Salvia officinalis leaves," Corrosion Science, vol. 62, no. pp. 122–135.

[31]. Talari **M.**, S.M. Nezhad, S.J. Alavi, M. Mohtashamipour, A. Davoodi, S. Hosseinpour, (2019) 'Experimental and computational chemistry studies of two imidazole-based compounds as corrosion inhibitors for mild steel in HCl solution, J. Mol. Liq. 286 110915, https://doi.org/10.1016/j.molliq.2019. 110915.

[32]. Tebbji K., N. Faska, A. Tounsi, and H. Oudda(2007)., "The effect of some lactones as inhibitors for the corrosion of mild steel in 1M hydrochloric acid," Materials Chemistry and Physics, vol. 106, no. 2–3, pp. 260–267.

[33]. Verma C., Quraishi .M.A, and Enzo E. Ebenso (2020) "Quinoline and its derrivatives as corrosion inhibitors; A Review, Surface and Interfaces, science direct Vol. 21(100634)

[34]. Vlad C. Sandu, IonelaDumbrava, Ana Maria Cormos, Arpad Imre-Lucaci, Calin C. Cormos, Paul D. Cobden, Robert de Boer (2019) " Computational Fluid Dynamics of Rectangular Monolith Reactor vs. Packed-Bed Column for Sorption-Enhanced Water-Gas Shift, Computer Aided Chemical Engineering, Vol 46, Pages 751-756

[35]. Wazzan NA, Obot I, Kaya S (2016) "Theoretical modeling and molecular level insights into the corrosion inhibition activity of 2-amino-1, 3, 4-thiadiazole and its 5-alkyl derivatives. J MolLiq. ;221:579. DOI: http://dx.doi.org/10.1016/j.molliq.2016.06.011

[36]. Wazzan NA. (2015) "DFT calculations of thiosemicarbazide, arylisothiocynates, and 1-aryl-2, 5-dithiohydrazodicarbonamides as corrosion inhibitors of copper in an aqueous chloride solution. Journal IndEng Chem. Vol.26291.DOI: http://dx.doi.org/10.1016/j.jiec.11.043

[37]. Xhanari and Finsgar (2016) 'Organic corrosion inhibitors for aluminium and its alloys in acid solutions, RSC Advances 6(67):62833-62857.

[38]. Yurt, A.,Ulutas, S. and Dal, H. (2006). Electrochemical and theoretical investigation on the corrosion of aluminium in acidic solution containing some Schiff bases. Applied Surface Science 253: 919–925.

[39]. Zhang H., Y. Chen, Z. Zhang, (2018) 'Comparative studies of two benzaldehydethiosemicarbazone derivatives as corrosion inhibitors for mild steel in 1.0 M HCl, Result Phys. 11) 554e563, https://doi.org/10.1016/j.rinp..09.038.

[40]. Zhao, P.,Liang, Q., and Li, Y. (2005). Electrochemical, SEM/EDS and quantum chemical study of phthalocyanines as corrosion inhibitors for mild steel in 1 mol/l HCl. Applied Surface Science 252: 1596–1607.

[41]. Zhu C., H. X. Yang, Y. Z. Wang, D. Q. Zhang, Y. Chen, and L. X. Gao (2018), "Synergistic effect between glutamic acid and rare earth cerium (III) as corrosion inhibitors on AA5052 aluminum alloy in neutral chloride medium," Ionics, vol. 25, no. 3, pp. 1395–1406,.